

# Quantifying high-order interdependencies on individual patterns via the local O-information: theory and applications to music analysis

Tomas Scagliarini,<sup>1</sup> Daniele Marinazzo,<sup>2</sup> Yike Guo,<sup>3,4</sup> Sebastiano Stramaglia,<sup>1,5</sup> and Fernando E. Rosas<sup>4,6,7</sup>

<sup>1</sup>*Dipartimento Interateneo di Fisica, Università degli Studi Aldo Moro, Bari and INFN, Italy*

<sup>2</sup>*Department of Data Analysis, Ghent University, Belgium*

<sup>3</sup>*Department of Computer Science, Hong Kong Baptist University, Hong Kong*

<sup>4</sup>*Data Science Institute, Imperial College London, United Kingdom*

<sup>5</sup>*Center of Innovative Technologies for Signal Detection and Processing (TIREs), Università degli Studi Aldo Moro, Italy*

<sup>6</sup>*Centre for Psychedelic Research, Department of Brain Science, Imperial College London, United Kingdom*

<sup>7</sup>*Centre for Complexity Science, Imperial College London, United Kingdom*

(Dated: August 27, 2021)

High-order, beyond-pairwise interdependencies are at the core of biological, economic, and social complex systems, and their adequate analysis is paramount to understand, engineer, and control such systems. This paper presents a framework to measure high-order interdependence that disentangles their effect on each individual pattern exhibited by a multivariate system. The approach is centred on the *local O-information*, a new measure that assesses the balance between synergistic and redundant interdependencies at each pattern. To illustrate the potential of this framework, we present a detailed analysis of music scores from J.S. Bach, which reveals how high-order interdependence is deeply connected with highly non-trivial aspects of the musical discourse. Our results place the local O-information as a promising tool of wide applicability, which opens new perspectives for analysing high-order relationships in the patterns exhibited by complex systems.

## I. INTRODUCTION

The analysis of interdependence is crucial for understanding the staggering complexity of structures and behaviours manifested in biological, economic and social systems. The unprecedented amount of data available for scientific scrutiny provides unique opportunities to deepen our understanding of multivariate co-evolving complex systems, including the orchestrated activity of multiple brain areas, the interactions between different genes, and the relationship between various econometric indices. Importantly, what allows these systems to be more than the sum of their parts is not to be found in the material nature of their parts, but in the fine structure of their interdependencies [1].

Information theory provides an ideal framework to study interdependencies in multivariate system, which establishes the notion of *information* as a common currency under which diverse systems can be measured and compared [2]. A particularly promising approach for analysing the structure of interdependencies is the partial information decomposition (PID), which distinguishes different ‘modes’ of information that multiple predictors convey about a target variable [3–5]. Two paradigmatic examples of such modes are synergy and redundancy [6–10]: redundancy corresponds to information which can be retrieved independently from more than one source, while synergy correspond to statistical relationships that exist in the whole but cannot be seen in the parts — this being rooted in the elementary fact that variables can be pairwise independent while being globally correlated.

Despite continuous efforts to develop PID, the precise way in which synergies and redundancies should be calculated is still being revised [11–24]. One way to circumvent this challenge is to avoid computing the full decomposition, and study mixtures of PID modes that

can be captured by linear combinations of Shannon measures. One such measure is the O-information [25], which has been shown to effectively capture the overall balance between redundant and synergistic modes. The effectiveness of the O-information in practical analyses has been verified by recent applications on populations of spiking neurons [26], and the relationship between neural patterns and ageing [27].

An important limitation of the O-information is that it characterises a multivariate system with a single number, which summarises to the aggregated effect of various patterns. Building on the rich literature of pointwise information measures [28–30], in this paper we introduce the *local O-information*, which evaluates each pattern separately — such that its ensemble average recovers the O-information. More specifically, the local O-information constitutes an overall measure that characterise the high-order interdependencies between the parts of a multivariate system at each possible pattern of activity. Put differently, the local O-information evaluates the ‘statistical quality’ of each pattern, providing a signed scalar that assesses the balance between redundancies and synergies at each individual pattern.

This paper presents the theory behind the local O-information, and then illustrates its rich capabilities by analysing the scores of the chorales of J.S. Bach. Our results show how the local O-information is capable of revealing subtle musical relationships, including properties of different intervals, chord dispositions, harmonic depth, and the relationship between music and text. Thanks to its ability to uncover such highly non-trivial relationships, the local O-information is a valuable addition to the toolkit of data analysts interested in the study of complex systems.

The rest of the paper is organised as follows. Section II provides background information about the O-

information, introduces the new local O-information, and then illustrates its basic properties on small spin systems. Then, Section III presents a detailed analysis of the local O-information on the chorales of J.S Bach, and finally Section VI summarises our main conclusions.

## II. A LOCAL MEASURE OF INFORMATION QUALITY

Let us consider a scientist who is interested in studying a given complex system, whose state can be appropriately described by the vector  $\mathbf{X}^n = (X_1, \dots, X_n)$ . We focus on scenarios where the scientist has enough data to build a reliable statistical description of the statistics of  $\mathbf{X}^n$ , which is denoted by  $p(\mathbf{X}^n)$ . A question of interest is how to leverage the statistics encoded in  $p$  in order to deepen our understanding of the structure of interdependencies that characterize  $\mathbf{X}^n$ . Such understanding can lead either to the building of statistical markers to classify different systems or different states of the same system, or to establish parallels between seemingly heterogeneous systems based on the similarity of their relational structure.

Through this section, random variables are denoted by capital letters (e.g.  $X, Y$ ) and their realisations by lower case letters (e.g.  $x, y$ ). Random vectors and their realisations are denoted by capital and lower case boldface letters, respectively.

### A. O-Information

Shannon's mutual information is a popular metric of interdependency, which overcomes the limitations of correlation metrics such as Pearson's in that it captures both linear and non-linear relationships and being applicable to ordinal data. However, the mutual information can only assess the relationships between two (sets of) variables, being unable to fully explore the rich interplay that can take place within triple or higher-order interactions.

Two multivariate extensions of the mutual information are the *Total Correlation* (TC) [31] and the *Dual Total Correlation* (DTC) [32], which are defined as

$$\begin{aligned} \text{TC}(\mathbf{X}^n) &:= \sum_{i=1}^n H(X_i) - H(\mathbf{X}^n), \\ \text{DTC}(\mathbf{X}^n) &:= H(\mathbf{X}^n) - \sum_{i=0}^N H(X_i | \mathbf{X}_{-i}^n). \end{aligned}$$

Above,  $H(X_i) = -\sum_{x_i} p(x_i) \log p(x_i)$  corresponds to the Shannon entropy,  $H(X_i | X_j) = H(X_i, X_j) - H(X_j)$  is the conditional Shannon entropy, and  $\mathbf{X}_{-i}^n$  is the vector of all variables except  $X_i$  (i.e.,  $\mathbf{X}_{-i}^n = (X_1, \dots, X_{i-1}, X_{i+1}, \dots, X_n)$ ); hence, the term  $H(X_i | \mathbf{X}_{-i}^n)$  quantifies how  $X_i$  is independent from the other  $n-1$  variables. As the mutual information, both TC and DTC are non-negative quantities which are zero if

and only if all variables  $X_0, \dots, X_N$  are jointly statistically independent — i.e. if  $p(\mathbf{X}^n) = \prod_{i=1}^n p(X_i)$ .

Despite the similarities between TC and DTC, these two metrics provide distinct but complementary views on the strength of the interdependencies in a multivariate system. On the one hand, the TC accounts for *collective constraints*, which refer to regions of the phase space that the system explore less; while on the other hand, the DTC measures the degree of *shared randomness* between the variables, i.e. the amount of information that can be collected in one variable that also refers to the activity of another [25]. An attractive way to exploit these complementary views is by considering their difference,

$$\Omega_n(\mathbf{X}^n) = \text{TC}(\mathbf{X}^n) - \text{DTC}(\mathbf{X}^n). \quad (1)$$

which is known as the *O-information* [25]. The O-information can be seen as a revision of the measure of neural complexity proposed by Tononi, Sporns and Edelman in [33], which provides a mathematical construction that is closer to their original desiderata [34]. In effect, the O-information is a signed metric that captures the balance between high- and low-order statistical constraints [35]. By construction,  $\Omega(\mathbf{X}^n) < 0$  implies a predominance of high-order constraints within the system  $\mathbf{X}^n$ , a condition that is usually referred to as *statistical synergy*. Conversely,  $\Omega(\mathbf{X}^n) > 0$  implies that the system  $\mathbf{X}^n$  is dominated by low-order constraints, which imply *redundancy* of information. This nomenclature is further supported by the following key properties:

- (1) It captures genuine high-order effects, at it is zero for systems with only pairwise interdependencies: if the joint distribution of  $\mathbf{X}^{n-1}$  (for  $n$  odd) can be factorised as  $p_{\mathbf{X}^{n-1}}(\mathbf{x}^{n-1}) = \prod_{k=1}^{n/2} p_{X_{2k}, X_{2k+1}}(x_{2k}, x_{2k+1})$ , then  $\Omega(\mathbf{X}^n) = 0$ .
- (2) The O-information is maximised by redundant distributions where the same information is copied in multiple variables, and is minimised by synergistic (“xor-like”) distributions: e.g. for binary variables,  $\Omega$  is maximised by the “n-bit copy” where  $X_1$  is a Bernoulli r.v. with parameter  $p = 1/2$  and  $X_0 = \dots = X_{N-1}$ , and is minimised when  $X_0, \dots, X_{N-2}$  are i.i.d. fair coins and  $X_{N-1} = \sum_{j=0}^{N-2} X_j \pmod{2}$ .
- (3) The O-information characterises the dominant tendency, being additive over non-interactive subsystems: if the system can be factorised as  $p_{\mathbf{X}^N}(\mathbf{x}^N) = p_{X_1, \dots, X_m}(x_1, \dots, x_m) \times p_{X_{m+1}, \dots, X_N}(x_{m+1}, \dots, x_N)$ , then  $\Omega(\mathbf{X}^n) = \Omega(X_1, \dots, X_{m-1}) + \Omega(X_m, \dots, X_n)$ .

For more details related to the O-information, we refer the reader to Ref. [25].

### B. Local O-Information

Building on the properties of the O-information reviewed in the previous section, one can design a measure

that can capture these effects on a state-by-state basis. In effect, the O-information provides a single scalar that characterises the interdependencies of a system *on average*. However, in many systems of interest this average represents a mid-point between highly heterogeneous states, which could potentially be of limited value to understand the role of individual patterns. In this section we introduce a *pointwise* measure that allows to calculate the O-information on individual states.

As a first step, let us introduce a *local total correlation* and *local dual total correlation* which are given by

$$\text{tc}(\mathbf{x}^n) := \sum_{j=1}^n h(x_j) - h(\mathbf{x}^n), \quad (2)$$

$$\text{dtc}(\mathbf{x}^n) := h(\mathbf{x}^n) - \sum_{j=1}^n h(x_j | \mathbf{x}_{-j}^n), \quad (3)$$

where  $h(\mathbf{x}^n) = -\log p(\mathbf{x}^n)$  is the information content of the state  $\mathbf{x}^n$  [28]. These quantities capture how the strength of the multivariate interdependencies vary with the state of the system, providing a generalisation to the pointwise mutual information introduced in Ref [36].

Using these definitions, we can define the *local O-information* as follows:

$$\omega(\mathbf{x}^n) := \text{tc}(\mathbf{x}^n) - \text{dtc}(\mathbf{x}^n) \quad (4)$$

$$= (n-2)h(\mathbf{x}^n) + \sum_{j=1}^n \left( h(x_j) - h(\mathbf{x}_{-j}^n) \right). \quad (5)$$

In contrast to  $\Omega(\mathbf{X}^n)$ , which provides a single value for the random variable,  $\omega(\mathbf{x}^n)$  assigns a number of each possible state  $\mathbf{x}^n$ . In particular, the local O-information has the following useful properties:

- $\Omega(\mathbf{X}^n) = \mathbb{E}\{\omega(\mathbf{x})\}$ .
- $\inf_{\mathbf{x}} \omega(\mathbf{x}) \leq \Omega(\mathbf{X}^n) \leq \sup_{\mathbf{x}} \omega(\mathbf{x})$ .

Generally speaking, the local O-information provides more information than its global counterpart as, technically,  $\omega(\mathbf{X}^n)$  is a random variable whose mean value is  $\Omega(\mathbf{X}^n)$ . Therefore, the whole range of values of  $\omega(\mathbf{X}^n)$  can naturally provide a more fine-grained description of the system than its mere first moment.

Additionally, note that Lemma 3 of Ref. [25] provides upper and lower bounds for  $\Omega(\mathbf{X})$  when the variables take values in a finite alphabet; in particular, if  $X_j \in \mathcal{X}$  for all  $j$  then

$$-(n-2) \log |\mathcal{X}| \leq \Omega(\mathbf{X}^n) \leq (n-2) \log |\mathcal{X}|. \quad (6)$$

Note that these bounds don't apply to the local O-information — they apply to its average value, but extreme values can be larger than it. Nonetheless, the quantity  $(n-2) \log |\mathcal{X}|$  establishes a natural bound which that, when surpassed, values of  $\omega$  can be considered to be particularly large. This provides a useful rule of thumb to interpret the ranges of values obtained by evaluations of  $\omega$ .

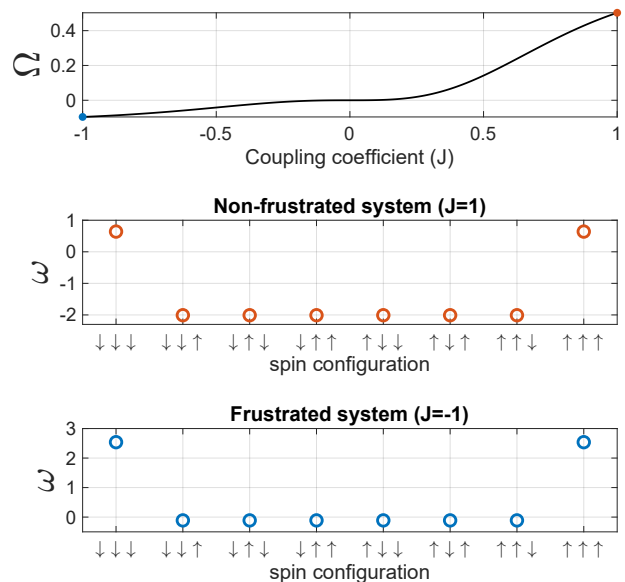


FIG. 1. Concerning the Ising toy model of three spins,  $\Omega$  is plotted versus the coupling  $J$  (top panel). The values of  $\omega$  for the 8 possible configurations of the three spins are shown for the unfrustrated case when  $J = 1$  (middle panel) and for the frustrated case, when  $J = -1$  (bottom panel).

### C. Proof of concept

An useful way of employing  $\omega$  is to classify states among different *types*. In particular, building on the properties of the O-information, we say that a state  $\mathbf{x}^n$  for which  $\omega(\mathbf{x}^n) > 0$  is redundancy-dominated, while if  $\omega(\mathbf{x}^n) < 0$  we say the state is synergy-dominated. In this section we illustrate this capability of the local O-information by using it to analyse a small Ising system.

Let's consider three coupled spins denoted by  $(S_1, S_2, S_3)$ , whose joint probability distributions follows a Boltzmann-Gibbs distribution of the form:

$$p(s_1, s_2, s_3) = \frac{e^{J(s_1 s_2 + s_1 s_3 + s_2 s_3)}}{Z}, \quad (7)$$

with  $Z = \sum_{s_1, s_2, s_3} e^{J(s_1 s_2 + s_1 s_3 + s_2 s_3)}$  is a normalisation factor. For positive values of  $J$ , the configurations with all the spins in agreement (i.e.  $\uparrow\uparrow\uparrow$  and  $\downarrow\downarrow\downarrow$ ) satisfy all bonds, and hence the system may be seen as a small ferromagnet. In contrast, for negative  $J$  the system is said to be “frustrated” as there is not a configuration satisfying all bonds simultaneously.

By analysing Eq. (7) via the O-information, one finds that ferromagnetic behaviour are redundancy-dominated while frustrated systems are synergy-dominated (see Figure 1). Interestingly, the local O-information shows that configurations of spin agreement are redundancy-dominated states, whilst the six configurations with disagreement are synergy-dominated — this for both positive and negative values of  $J$ . This let us conclude that what makes the system redundancy- or synergy-dominated for different values of  $J$  is the different

frequency with which either redundancy- or synergy-dominated configurations are visited.

This toy example shows how the local O-information can reveal different qualities of various states — in this case, either states with agreement or disagreement. Furthermore, this example also reveals an intriguing connection between synergy and frustration in spin models, which will be further investigated in a future publication.

### III. CASE STUDY: HIGH-ORDER RELATIONSHIPS IN BACH'S CHORALES

To illustrate the usefulness of the local O-information for practical data analysis, this section presents a study of the multivariate statistics of musical scores from the Baroque period. Ref. [25] provided an analysis of music scores based on the global O-information; however, such analyses could not provide information about individual chords, and hence could not explore further musical aspects related to harmony and tonality. Here we show how the local O-information can greatly expand this type of analyses, revealing subtle aspects of the musical discourse that are reflected in the high-order interactions.

In the following, Section III A describes the procedure to obtain and analyse the data, and Section III B discusses our main findings.

#### A. Processing pipeline

##### 1. Data

Our analysis focuses on the chorales for four voices (soprano, alto, tenor, and bass) written by Johann Sebastian Bach (1685-1750). These works are characterised by an elaborate counterpoint between the melodic lines that leads to rich harmonic progressions, which in turn results into a broad range of chords displayed along the repertoire. An additional point of interest of these pieces is that, as typical in the Baroque period (approx. 1600–1750), they display a balance in the interest and richness of each of the four voices. This contrasts with the subsequent Classic (1730–1820) and Romantic (1780–1910) periods, where higher voices tend to take the lead while the lower voices provide mere support.

Our analysis is based on the electronic scores publicly available at <http://kern.ccarh.org>, a website that hosts professionally curated digital scores [37]. Our pre-processing pipeline is the same as in Ref. [25], which we describe here for completeness. The scores were pre-processed in Python using the Music21 package (<http://web.mit.edu/music21>), which allowed us to select only the pieces written in Major mode. Each chorale was transposed to *C Major*, and each melodic line was transformed into time series of 13 possible values (one for each note plus one for the silence), using a small rhythmic duration as common time unit. This resulted in a total of 172 chorales, which gave  $\approx 4 \times 10^4$  four-note chords.

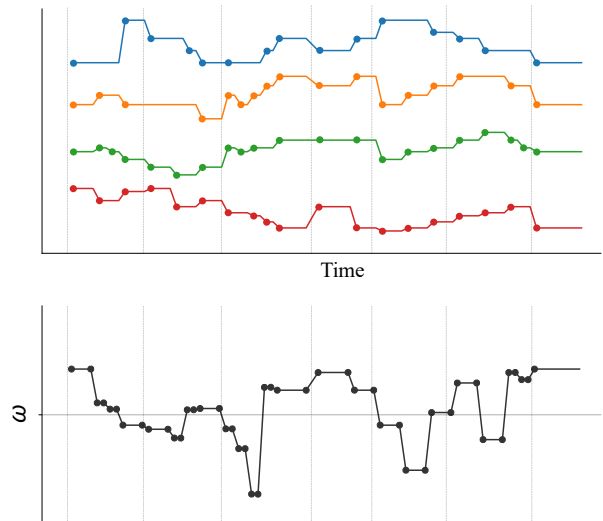


FIG. 2. **Processing pipeline** *Top*: each chorale was selected among those written in major mode and then transposed in C major. *Middle*: each melodic line was transformed into a time series of 13 possible values. *Bottom*: for each 4-note state the local O-information was calculated using Eq. (5).

With this data, the joint distribution of the values for the four-note chords was estimated using their empirical frequency [38]. This leads to a probability assigned to each four-note chord, which assess simply the odds of picking that chord when randomly selecting one out of the whole repertoire. One can express this probability as the multivariate statistic  $p(x_1, x_2, x_3, x_4)$ , with each variable corresponding to the different voices.

Finally, we used  $p(x_1, x_2, x_3, x_4)$  to calculate the local O-information  $\omega(\mathbf{x})$  for each chord  $\mathbf{x}$  using Eq. (5), which determines the dominant statistical behaviour (in terms of synergy and redundancy) associated with each chord. The overall pipeline starting from the music score and arriving to the local O-information is illustrated in Figure 2.

##### 2. Research questions and tools

We studied the multivariate properties of each of the possible four-note chords of Bach's chorales. Our analysis focuses exclusively on harmony and chords, leaving melodic and rhythmic properties to future studies. We focus on the question of what harmonic properties of the

music tend to give rise to synergistic or redundant high-order relationships between the four voices.

Let us denote by  $\mathbf{X} = (X_1, X_2, X_3, X_4)$  the random vector that follow the statistics encapsulated by  $p(x_1, x_2, x_3, x_4)$ . Following standard musical practice, we follow the convention that the variables go from lower to higher range, so that  $X_1$  corresponds to the bass and  $X_4$  is the soprano. Moreover, we use the shorthand notation **CEGE** when referring to the chord  $(x_1, x_2, x_3, x_4) = (\text{C}, \text{E}, \text{G}, \text{E})$ .

Note that  $\mathbf{X}$  can adopt  $13^4 = 28561$  possible values, and that  $p$  is generally not invariant under changes of ordering between the four voices. Since  $X_1, \dots, X_4$  take values among alphabets of cardinality  $|\mathcal{X}| = 13$ , we do all calculations using logarithms to base 13, so that  $H(X_k) \leq 1$  for all  $k \in \{1, \dots, 4\}$  — we call this unit a *mut*, for *musical bit*. Eq. (6) implies that  $-2 < \Omega(\mathbf{X}) < 2$ , and hence most values of  $\omega$  are expected to have absolute value less than 2 muts — which gives a sense of how to interpret the magnitude of local O-information values.

We expected to find a correspondence between tonality and O-information values. In particular, we hypothesise that the principal tonal chords (**C**, **F**, and **G** major) would be associated with redundant behavior, while chords that are farther away from the tonal centre (i.e. involve many sharp or flat alterations) would be related to synergistic events. Additionally, we expect dissonance to be associated with less redundancy, as it involves more complex combinations of notes.

## B. Results

### 1. Analysis of the extreme values of the local O-information

Out of the  $13^4$  possible chords, we found that only 1715 of them were observed at least once in the chorales, corresponding to only 6% of the possibilities — reflecting the specificity of the chord choices used in Bach’s chorales. A weak correlation is observed between frequency and local O-information: more frequent chords tend to have a higher  $\omega$  — which suggests that more visited chords tend to be made by more redundant parts (see Figure 3). The most frequently encountered chords are shown in the Appendix (Table IV).

Some interesting observations can be made by observing the most positive (redundant) and the most negative (synergistic) states in terms of  $\omega$ , which are presented in Table I. On the one hand, the most redundant states tend to contain few alterations (sharp notes, denoted in the table with the symbol  $\sharp$ ) and mostly consonant intervals [39]. In contrast, synergistic chords tend to contain more alterations and dissonant intervals, which in the Western culture are typically associated with harshness and unpleasantness. For example, the most synergistic

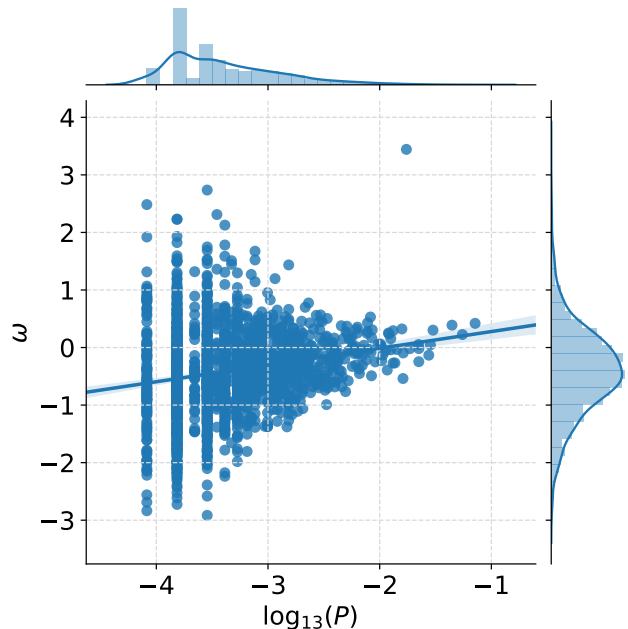


FIG. 3. Scatter plot of the logarithm of the probability of each state versus  $\omega$ . Almost all the states have  $\omega$  between  $-2$  and  $+2$  — i.e. the bounds for  $\Omega$ . The outlier in redundancy corresponds to the chord **RRRR**.

chord contains a major seconds (**D-E**), while the second most synergistic has one minor second (**F $\sharp$ -G**) and one major second (**E-F $\sharp$** ). The “chord” with highest local O-information is found to be **RRRR**, where the redundancy can be interpreted as a consequence of the voices doing the same thing — not signing.

### 2. The role of intervals

The results reported in the previous section imply a link between the musical (harmonic) properties of a chord and the type of the statistical interdependencies within it constituent notes. In particular, results suggest that synergistic interdependencies may be linked to the presence of dissonances, while redundancy may be related to consonance. A consonant interval occurs when the ratio of the frequencies between two notes is very simple, like  $(1:2)$  for the octave,  $(2:3)$  for the perfect fifth or  $(4:5)$  for the major third. In the Western culture, consonance is typically associated by listeners with pleasantness and acceptability [40]. In Westerner music theory, dissonant intervals typically include the major second  $(8:9)$  and minor second  $(15:16)$ , major seventh  $(8:15)$  and minor seventh  $(9:16)$ , and the augmented fourth (so-called ‘tritone’ or *diabolus in musica*).

To further explore the relationship between high-order statistics and harmony, we studied how the local O-information depends on the number of dissonant intervals (either seconds/sevenths or augmented fourths) a chord possesses. The results are depicted in Figure 4. Analysis

Redundancy		Synergy	
Chord	$\omega$	Chord	$\omega$
R R R R	3.443	A E D D	-2.916
G D G D	2.736	G B F# E	-2.836
F C F C	2.484	B F B B	-2.725
A C A C	2.311	A# E E A	-2.688
C G C C	2.23	G F# F# A	-2.613
E G E G	2.228	G C B A	-2.581
C G C G	2.127	F A# G F	-2.559
A A E A	1.93	G C C A#	-2.522
F D G D	1.921	G E C# A	-2.432
D D A A	1.824	G G G# C	-2.396
G D G G	1.782	R G R E	-2.388
D D A D	1.748	G# F G# C	-2.311
D F C A	1.688	A# F G# C	-2.276
G G D G	1.674	G A F G	-2.245
F F C F	1.594	E G A F	-2.238
E C E C	1.586	E F# C D	-2.221
A C A D	1.544	F# F# C# A	-2.219
F F C D	1.532	G F F A#	-2.185
R R R A	1.522	E A G D	-2.176
G F G D	1.512	C# G G B	-2.173

TABLE I. Chords with the highest (redundance) and lowest (synergy) local O-information. Letters refers to the standard music nomenclature (plus R is for silence), and the ordering of the voices is Bass-Tenor-Alto-Soprano — from left to right.

of variance with Bonferroni correction revealed a significant dependency between number of dissonances and  $\omega$  for all number of chords — except for the contrast between 3 and 4 dissonances, arguably due to the small number of chords with 4 dissonances. The results of all the comparison are shown in Table II. The chords that

Dissonances	$p$ -value	Cohen's $d$
0-2	< 0.0001	0.738
0-3	< 0.0001	1.187
0-4	< 0.0001	1.556
1-2	< 0.0001	0.317
1-3	< 0.0001	0.821
1-4	< 0.0001	1.272
2-3	< 0.0001	0.488
2-4	0.0004	0.924
3-4	0.5865	0.447

TABLE II.

contain 3 or more dissonant intervals are presented in the Appendix (Table VII), most of which exhibits negative values of  $\omega$ . Remarkably, the only two chords of those with  $\omega > 0$  can be identified as part of G major with added 7-th, which is the most frequent dissonant chord in classical harmony.

A question that raises from the results shown in Figure 4 is why purely consonant chords can be dominantly synergistic, as shown by the variance of the values of  $\omega$  for zero dissonance. For example, the chord  $\omega(\text{CEGC}) = 0.42$  is redundant while  $\omega(\text{EGCC}) = -0.45$ , being both C major chords but having a different pitch in the bass (the fundamental note in the first case, and the third in the second). Leveraging music theory, an explanation from

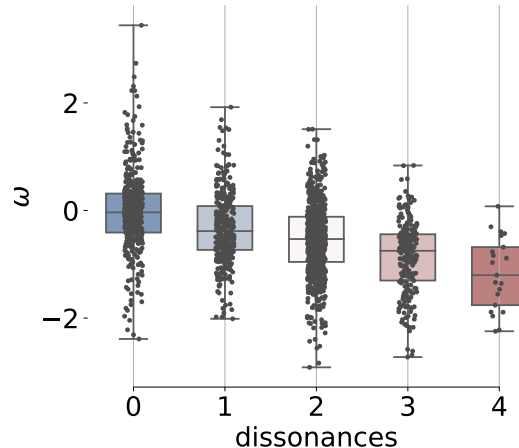


FIG. 4. Dissonance vs local O-information. Each box represents a state with a different number of dissonant interval. Each category is statistically different from the one with no dissonance (pure consonant intervals).

this comes from the notion of ‘chord inversion:’ a triad chord is in *first inversion* if the third (either major or minor) is in the bass, it is in *second inversion* if the fifth is in the bass, and it is in *root position* if the first/fundamental note is in the bass. In Western classical music each inversion tends to be associated with specific sensations – the first inversion gives a sense of lightness, while the second inversion and root position are typically associated with instability and stability, respectively. By considering the values of  $\omega$  corresponding to different inversions, t-test shows a tendency towards lower values of  $\omega$  in chords in first (Cohen’s  $d \simeq 0.36$ ) and second (Cohen’s  $d \simeq 0.31$ ) inversion when compared to chords in root position, as shown in Figure 5.

Finally, as a complementary way to study the role of intervals on the O-information, we considered the average value of  $\omega$  for given notes at specific voices — averaging over all possible notes adopted by the other two voices. Results are shown in Figure 6. It was found that redundancy (i.e. the most positive values of O-information) is ‘localised’ in few intervals, taking place mainly between notes involving the tonic (C major, CEG) or dominant (G major, GBD) chords, or between silences. Also, most redundancy in the bass is associated to the fundamental note of each chord — either C or G. In contrast, synergy (i.e. the most negative values of O-information) are much more widespread. Interestingly, the redundancies between the two extreme voices (soprano and bass) are relatively weak (except between their silence), while synergies between them are not. Please note that the extreme voices tend to carry an important role in Bach chorales — the soprano carrying out the main melody, and the bass leading the harmony.

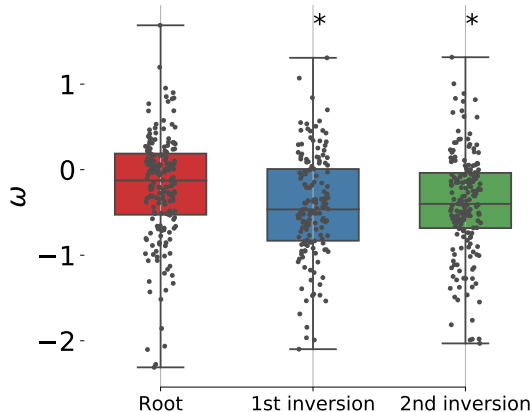


FIG. 5. **The effect of chords inversions on the local O-information.** Root form occurs when the root note of the triad is in the bottom (e.g. CEG), first inversion when the third of the triad is the bass note (e.g. EGC), and second inversion when the fifth is in the bass (e.g. GCE).

### 3. Harmonic depth

While the previous section focused on the role of single intervals, now our analyses focuses on harmonic considerations. Harmony is organised around a *tonality* (also called ‘key’), which plays the role of centre of gravity around which music discourse revolves. The axial pitch of a tonality is called the *root*, which in turn gives name to the tonality — e.g. C is the root of the tonality of C major. In classical Western music there are 12 different major tonalities, one for each of each pitch. Also, each major tonality has an associated minor tonality, which is located a minor third below (e.g. C major is associated with A minor). Each of these 12 major tonalities are made of 7 distinct pitches, and are naturally ordered by a notion of proximity depending on how many pitches do they have in common. This gives raises to the *circle of fifths*: major keys separated by a fifth have only one note different. For example, C and G major are only distinguished by the note F, which is sharp for the latter but natural for the former.

A simple way to explore the impact of harmony on the high-order statistics is by analysing the dependency between  $\omega$  and the number of alterations (sharps or flats) that a chord has. In effect, please recall that all the chorales analysed are in major mode, and have been shifted to C (see Section III A). Moreover, chords belonging to C major have no alterations, while chords for more distant tonalities have progressively more alterations — either sharps if going up the cycle of fifths, or flats otherwise. Therefore, we ran statistical analyses (t-test corrected for multiple comparisons) on the effect of the number of alterations on  $\omega$ , whose results are shown in Figure 7. Results revealed significantly decreases of

$\omega$  ( $p < 0.01$ ) for states with one (Cohen’s  $d \simeq 0.41$ ) or two (Cohen’s  $d \simeq 0.44$ ) alterations with respect to chords without any alterations.

In order to go deeper into the impact of harmony on the O-information we introduced the notion of *harmonic depth*, which corresponds to the smallest number of steps (going clockwise or anti-clockwise) in the circle of fifths are required to go from C major to a given tonality — or from A minor, in case of minor tonality. For example, the chord D major has an harmonic depth of +2, while the chord F minor (denoted as Fm) has an harmonic depth of +4.

We are interested to study the relationship between  $\omega$  and harmonic depth. For this purpose, we consider the values of  $\omega$  for triads that belong to a specific tonality, regardless to the arrangement of notes between the voices. For example, determining a chord is C just accounts for triads containing only the pitches C, E, G, regardless how they are arranged among the voices. Results are shown in Figure 8, and show that the value of  $\omega$  decreases as soon as the tonality moves away from C major, being this difference more pronounced in minor chords. This suggest that synergy may also be associated with more complex harmonic explorations involving more harmonically distant chords.

### 4. Lyric analysis

As a final step in our analysis, we investigated the relationship between the values of  $\omega$  due to the chords and the corresponding word that is sang as part of the lyrics. For this purpose, we consider the different values of  $\omega$  that correspond to each time a given word is sang. In cases of melismas (i.e. when many notes are sang under the same syllable), the values of the whole progression were averaged and counted as one realisation of the word.

As a first analysis, we calculated a word cloud where words associated with negative or positive values of  $\omega$  are represented in red and blue, respectively. As shown in Figure 9, many of the most common words (like *Gott*, *Herr*, *Sohn*) are redundant, with the exception of *Jesu* that is synergistic. As the majority of the chords explored by Bach are synergistic (the average O-information is negative, see Figure 3), this prevalence of redundant words is highly non-trivial.

Another insight that can be drawn from the word cloud is that words that are not the subject of the phrase seems to be more synergistic. To verify this, we evaluated the effect on  $\omega$  of words being in root form (nominative case) with respect to all others [41]. Results confirmed our conjecture, showing that words in root form have a tendency towards higher values of  $\omega$  (see Figure 10). As an speculation, this may be interpreted by noting that root form words correspond to the most important part of the sentence, and hence a redundant underlying harmony might contribute to a easier comprehension. The most frequent cases of words for which we found both the root and the non root word are shown in Table III.

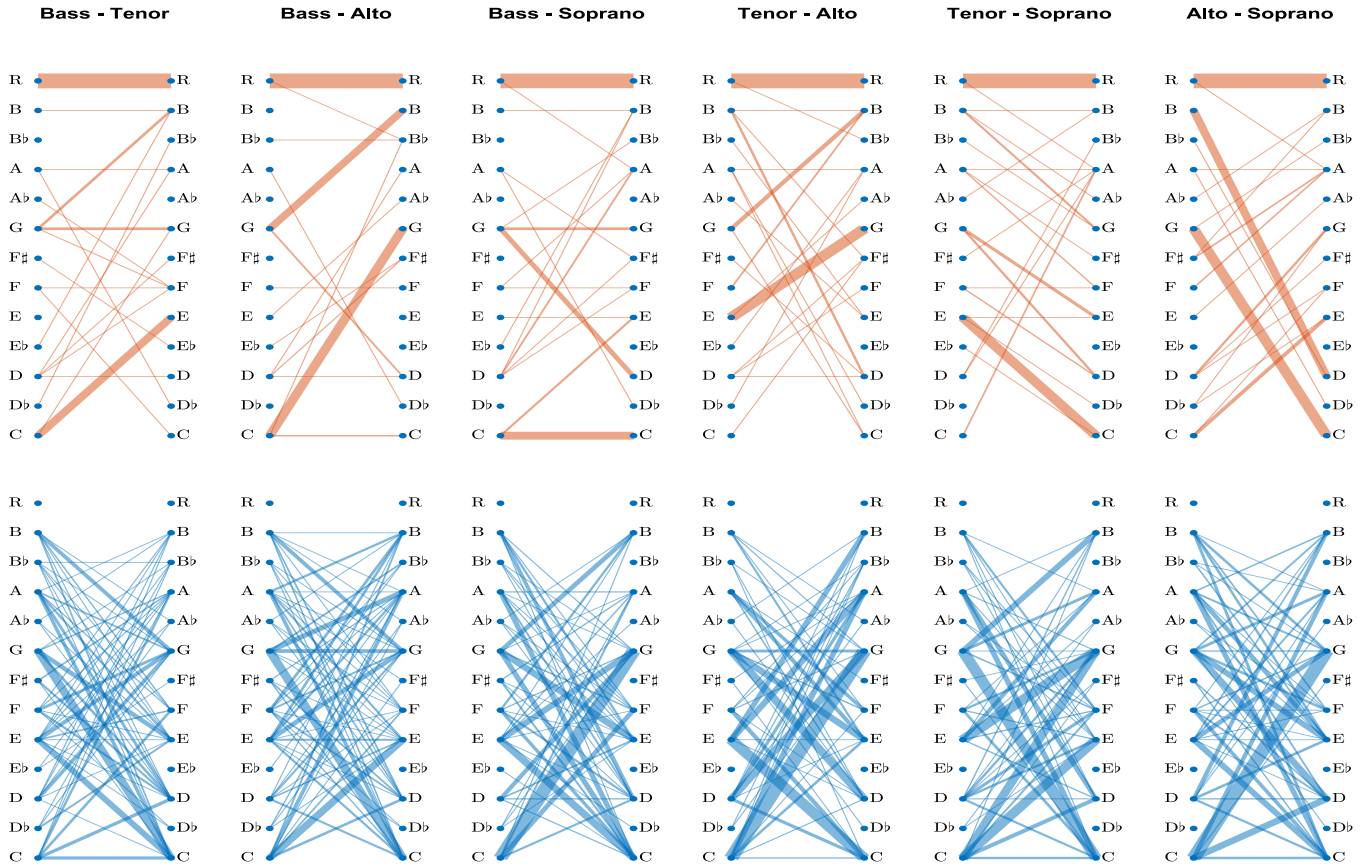


FIG. 6. Networks of redundant (orange) and synergy-dominated (blue) relationships in Bach's chorales. For each voice pair the links were created by averaging the local O-information of all chords that contain that pair of notes.

#### IV. CONCLUSIONS

This paper introduces a new framework to study the high-order interdependencies observed in complex multivariate systems, which is capable of disentangling their effects on individual patterns of activity. The approach is centred on the local O-information, a measure that quantifies the balance between redundancy and synergy at each pattern. Because of its information-theoretic nature, this measure is widely applicable — being suitable to assess systems with categorical, discrete, and continuous variables.

The capabilities of the proposed framework were showcased in an analysis of the scores of the chorales of J.S. Bach, which illuminated the high-order relationships that exist between the different voices. In particular, our results synergy-dominated interdependencies tend to be associated with complex musical elements, including dissonances, chord inversions, and harmonic distance from the tonal centre. Taken together, our findings provide converging evidence about the relationship between statistical synergy and the complexity of the musical discourse.

These findings have interesting parallels with recent studies on the human brain, which are revealing a close relationship between synergistic interdependencies in neural activity and high cognitive functions. Histori-

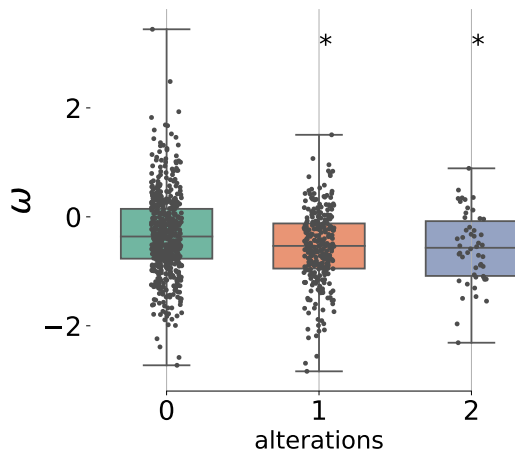


FIG. 7. The local O-information is related to the number of alterations (sharps and flat notes) inside each state. States with 1 and 2 alterations have  $\omega$  significantly lower ( $p < 0.05$ ) than states with no alterations.



of emergent phenomena, which have been recently characterised formally in terms of statistical synergy [47]. This would not be the first time music is shown to share some of the hallmark properties of complex systems; in effect, properties of musical discourse has been shown to be related to non-linear fluctuations and self-organised criticality [48, 49], and also to entropy production and irreversibility [50].

Pointwise information measures, initially proposed in Ref. [29] w.r.t. the local transfer entropy, are a promising set of techniques that can provide a detailed description of information transfer mechanisms in complex systems. Recently this paradigm has been applied to implement the local Granger causality [30], which has shown interesting results on physiological and neural data. The fine descriptions allowed by the formalism introduced in this paper bring a new perspective over high-order interdependencies, which complement existent pointwise information decomposition approaches (e.g. Ref. [51]) by being applicable to larger systems — hence greatly extending their domain of practical applicability. The extension of these ideas to dynamical information decomposition, such as the integrated information decomposition framework [52], constitutes a promising direction for future research.

#### ACKNOWLEDGEMENTS

The authors thank Pablo Padilla and Alejandro Reyes for insightful discussions. T.S. wants to thank M. Paolo Daniele for having transmitted to him a bit of his passion for music. F.R. was supported by the Ad Astra Chandaria foundation. S.S. was supported by MIUR project PRIN 2017WZFTZP “Stochastic forecasting in complex systems”.

#### CODE AVAILABILITY

Code for the analysis reported here is publicly available at [https://github.com/tomscag/local\\_0\\_information](https://github.com/tomscag/local_0_information)

## Appendix A: Tables

Chord	$\omega$	Frequency
C E G C	0.4201	1881
C G C E	0.226	1405
G G B D	0.3887	1106
G B D G	0.3019	715
G B G D	0.0464	674
C C G E	-0.1328	649
G D B G	-0.0182	517
C G E C	-0.2457	516
A E A C	0.0517	514
G D G B	-0.0189	421
R R R R	3.4431	388
E G C G	-0.0938	361
C E C G	-0.5384	359
G F B D	0.3229	350
B D G D	-0.0342	311
E C G C	-0.2682	298
E G C E	0.2924	286
C C E G	-0.2694	286
B G D G	-0.0387	272
D A D F	0.1538	271
A A C F	0.2383	260
F C F A	0.2522	257
G G C D	-0.3909	250
F F C A	-0.058	241
F F A C	-0.1293	226
F A C D	-0.2281	220
D F A D	0.0358	217
A A C E	0.0617	214
A C E C	0.0578	203
A A E C	-0.2498	190
C E G E	0.307	177
F A C F	0.1666	175
G G D B	-0.491	174
B G D F	-0.0853	172
D D F# A	0.5305	170

TABLE IV. Most common chords.

Redundancy		Synergy	
Chord	$\omega$	Chord	$\omega$
R R R R	3.443	A E D D	-2.916
G D G D	2.736	G B F# E	-2.836
F C F C	2.484	B F B B	-2.725
A C A C	2.311	A# E E A	-2.688
C G C C	2.23	G F# F# A	-2.613
E G E G	2.228	G C B A	-2.581
C G C G	2.127	F A# G F	-2.559
A A E A	1.93	G C C A#	-2.522
F D G D	1.921	G E C# A	-2.432
D D A A	1.824	G G G# C	-2.396
G D G G	1.782	R G R E	-2.388
D D A D	1.748	G# F G# C	-2.311
D F C A	1.688	A# F G# C	-2.276
G G D G	1.674	G A F G	-2.245
F F C F	1.594	E G A F	-2.238
E C E C	1.586	E F# C D	-2.221
A C A D	1.544	F# F# C# A	-2.219
F F C D	1.532	G F F A#	-2.185
R R R A	1.522	E A G D	-2.176
G F G D	1.512	C# G G B	-2.173
F G C D	1.508	G A C# A	-2.173
F# A C A	1.506	A D# A D	-2.144
B G B G	1.5	E E F# A	-2.143
C C G A	1.482	F# B E E	-2.142
F A A F	1.46	A G A# F	-2.115
G B G B	1.446	F A C# G	-2.114
C C G C	1.435	F B G# C	-2.103
G G D D	1.361	F# E B D	-2.099
G F A D	1.318	G E D A#	-2.09
C A D E	1.315	C# E F# B	-2.086

TABLE V. Table shows the first states with the highest (redundance) and lowest (synergy)  $\omega$  values. The letters refers to the standard nomenclature of notes in music (R is for rest) and the order of the voices is Bass-Tenor-Alto-Soprano, from left to right.

Chord	$\omega$	Occurrence
C E G C	0.42	1881
C G C E	0.226	1405
C C G E	-0.133	649
C G E C	-0.246	516
E G C G	-0.094	361
C E C G	-0.538	359
E C G C	-0.268	298
E G C E	0.292	286
C C E G	-0.269	286
C E G E	0.307	177
E G C C	-0.452	132
E C G G	-0.302	122
E C G E	0.015	113
E G G C	-0.577	102
E E G C	0.37	99
G G C E	0.149	90
E E C G	0.002	78
E G E C	-0.045	74
E C E G	0.093	71
E C C G	-0.467	52
C C E C	0.442	52
C C E E	0.033	44
C E C E	0.774	41
C G E G	-0.106	37
G G E C	-0.812	35
G E C E	-0.977	26
C C G C	1.435	26
E E G G	-0.16	25
C G E E	0.538	24
G E C C	-1.132	22

TABLE VI. Most common tonal chords.

Chord	$\omega$	Occurrence
G G B F	-0.2391	81
D D F# C	-0.4532	28
G F G B	-0.8748	27
C A# C E	-0.1148	27
D D C F#	-0.5139	26
G G F B	-0.8308	25
G F B G	0.226	25
G B G F	-0.7421	24
B A C F	-0.455	22
E F B D	-0.3088	22
D F# D C	-0.713	18
D C D F#	-0.7643	17
E D G# E	-0.262	17
B C A F	-0.7095	16
G B F G	0.2502	16
E F B G	-0.4072	14
C C E A#	-0.2633	14
C E D E	-0.7414	13
G F B C	-0.8746	12
D F C E	-0.5583	12
C D F# D	-1.0235	10
E E D G#	-0.7605	10
D C F# D	-0.1526	10
F B F A	-0.1821	9
B C F C	-1.8124	8
G F A# A	-1.5336	8
E D E G#	-0.7108	8
A E A# C	-0.6605	8
F G C# E	-0.5848	8
B C F A	-0.5059	8

TABLE VII. Most common dissonant chords (only chords with 3 or more dissonant intervals are shown).

- [1] James P. Crutchfield. The calculi of emergence: computation, dynamics and induction. *Physica D: Nonlinear Phenomena*, 75(1-3):11–54, 1994. Publisher: Elsevier.
- [2] James P. Crutchfield and David P. Feldman. Regularities unseen, randomness observed: Levels of entropy convergence. *Chaos: An Interdisciplinary Journal of Nonlinear Science*, 13(1):25–54, 2003. Publisher: American Institute of Physics.
- [3] Paul L. Williams and Randall D. Beer. Nonnegative decomposition of multivariate information. *arXiv preprint arXiv:1004.2515*, 2010.
- [4] Virgil Griffith. *Quantifying synergistic information*. California Institute of Technology, 2014.
- [5] Joseph T. Lizier, Nils Bertschinger, Jürgen Jost, and Michael Wibral. Information decomposition of target effects from multi-source interactions: Perspectives on previous, current and future work, 2018.
- [6] Itay Gat and Naftali Tishby. Synergy and redundancy among brain cells of behaving monkeys. *Advances in neural information processing systems*, pages 111–117, 1999. Publisher: MIT; 1998.
- [7] Elad Schneidman, William Bialek, and Michael J. Berry. Synergy, redundancy, and independence in population codes. *Journal of Neuroscience*, 23(37):11539–11553, 2003. Publisher: Soc Neuroscience.
- [8] Nicholas Timme, Wesley Alford, Benjamin Flecker, and John M. Beggs. Synergy, redundancy, and multivariate information measures: an experimentalist’s perspective. *Journal of computational neuroscience*, 36(2):119–140, 2014. Publisher: Springer.
- [9] Fernando Rosas, Vasilis Ntranos, Christopher J. Ellison, Sofie Pollin, and Marian Verhelst. Understanding interdependency through complex information sharing. *Entropy*, 18(2):38, 2016. Publisher: Multidisciplinary Digital Publishing Institute.
- [10] Michael Wibral, Viola Priesemann, Jim W. Kay, Joseph T. Lizier, and William A. Phillips. Partial information decomposition as a unified approach to the specification of neural goal functions. *Brain and cognition*, 112:25–38, 2017. Publisher: Elsevier.
- [11] Malte Harder, Christoph Salge, and Daniel Polani. Bivariate measure of redundant information. *Physical Review E*, 87(1):012130, 2013. Publisher: APS.
- [12] Virgil Griffith, Edwin KP Chong, Ryan G. James, Christopher J. Ellison, and James P. Crutchfield. Intersection information based on common randomness. *Entropy*, 16(4):1985–2000, 2014. Publisher: Multidisciplinary Digital Publishing Institute.
- [13] Adam B. Barrett. Exploration of synergistic and redundant information sharing in static and dynamical Gaussian systems. *Physical Review E*, 91(5):052802, 2015. Publisher: APS.
- [14] Eckehard Olbrich, Nils Bertschinger, and Johannes Rauh. Information decomposition and synergy. *Entropy*, 17(5):3501–3517, 2015. Publisher: Multidisciplinary Digital Publishing Institute.
- [15] Robin AA Ince. The Partial Entropy Decomposition: Decomposing multivariate entropy and mutual information via pointwise common surprisal. *arXiv preprint arXiv:1702.01591*, 2017.
- [16] Conor Finn and Joseph T. Lizier. Pointwise partial information decomposition using the specificity and ambiguity lattices. *Entropy*, 20(4):297, 2018. Publisher: Multidisciplinary Digital Publishing Institute.
- [17] Ryan G. James, Jeffrey Emenheiser, and James P. Crutchfield. Unique information via dependency constraints. *Journal of Physics A: Mathematical and Theoretical*, 52(1):014002, 2018. Publisher: IOP Publishing.
- [18] Ryan G. James, Jeffrey Emenheiser, and James P. Crutchfield. Unique information and secret key agreement. *Entropy*, 21(1):12, 2019. Publisher: Multidisciplinary Digital Publishing Institute.
- [19] Nihat Ay, Daniel Polani, and Nathaniel Virgo. Information decomposition based on cooperative game theory. *arXiv preprint arXiv:1910.05979*, 2019.
- [20] Fernando E. Rosas, Pedro AM Mediano, Borzoo Rasouli, and Adam B. Barrett. An operational information decomposition via synergistic disclosure. *Journal of Physics A: Mathematical and Theoretical*, 53(48):485001, 2020. Publisher: IOP Publishing.
- [21] Conor Finn and Joseph T. Lizier. Generalised measures of multivariate information content. *Entropy*, 22(2):216, 2020. Publisher: Multidisciplinary Digital Publishing Institute.
- [22] Aaron J. Gutknecht, Michael Wibral, and Abdullah Makkeh. Bits and pieces: Understanding information decomposition from part-whole relationships and formal logic. *Proceedings of the Royal Society A*, 477(2251):20210110, 2021. Publisher: The Royal Society Publishing.
- [23] Kyle Schick-Poland, Abdullah Makkeh, Aaron J. Gutknecht, Patricia Wollstadt, Anja Sturm, and Michael Wibral. A partial information decomposition for discrete and continuous variables. *arXiv preprint arXiv:2106.12393*, 2021.
- [24] Abdullah Makkeh, Aaron J. Gutknecht, and Michael Wibral. Introducing a differentiable measure of pointwise shared information. *Physical Review E*, 103(3):032149, 2021. Publisher: APS.
- [25] Fernando E. Rosas, Pedro AM Mediano, Michael Gastpar, and Henrik J. Jensen. Quantifying high-order interdependencies via multivariate extensions of the mutual information. *Physical Review E*, 100(3):032305, 2019. Publisher: APS.
- [26] Sebastiano Stramaglia, Tomas Scagliarini, Bryan C. Daniels, and Daniele Marinazzo. Quantifying dynamical high-order interdependencies from the  $\alpha$ -information: an application to neural spiking dynamics. *Frontiers in Physiology*, 11:1784, 2021. Publisher: Frontiers.
- [27] Marilyn Gatica, Rodrigo Cofré, Pedro AM Mediano, Fernando E. Rosas, Patricio Orío, Ibai Diez, Stephan P. Swinnen, and Jesus M. Cortes. High-order interdependencies in the aging brain. *Brain connectivity*, 2021. Publisher: Mary Ann Liebert, Inc., publishers 140 Huguenot Street, 3rd Floor New . . .
- [28] Terry Bossomaier, Lionel Barnett, Michael Harré, and Joseph T. Lizier. Transfer entropy. In *An introduction to transfer entropy*, pages 65–95. Springer, 2016.
- [29] Joseph T. Lizier, Mikhail Prokopenko, and Albert Y. Zomaya. Local information transfer as a spatiotemporal filter for complex systems. *Physical Review E*, 77(2):026110, 2008. Publisher: APS.
- [30] Sebastiano Stramaglia, Tomas Scagliarini, Yuri Antonacci, and Luca Faes. Local granger causality. *Physical*

- Review E*, 103(2):L020102, 2021. Publisher: APS.
- [31] Satoshi Watanabe. Information theoretical analysis of multivariate correlation. *IBM Journal of research and development*, 4(1):66–82, 1960. Publisher: IBM.
- [32] Han Te Sun. Nonnegative entropy measures of multivariate symmetric correlations. *Information and Control*, 36:133–156, 1978. Publisher: Elsevier.
- [33] Giulio Tononi, Olaf Sporns, and Gerald M. Edelman. A measure for brain complexity: relating functional segregation and integration in the nervous system. *Proceedings of the National Academy of Sciences*, 91(11):5033–5037, 1994. Publisher: National Acad Sciences.
- [34] For a comparison between the original measure proposed in Ref. [33] and the O-information, please see Ref. [25].
- [35] While low-order constraints impose strong restrictions on the system and allow little amount of shared information between variables, high-order constraints impose collective restrictions that enable large amounts of shared randomness.
- [36] Robert M Fano. *Transmission of information: a statistical theory of communications*. Mit Press, 1968.
- [37] Craig Stuart Sapp. Online database of scores in the humdrum file format. In *ISMIR*, pages 664–665, 2005.
- [38] Please note that regularisation methods — such as Laplace smoothing — can have significant effects on the results. We decided not to use such methods, as some chords (e.g. C-C♯-D-D♯) are not representative of the Baroque repertoire.
- [39] For a description of consonant and dissonant intervals, please see next section.
- [40] Imre Lahdelma and Tuomas Eerola. Cultural familiarity and musical expertise impact the pleasantness of consonance/dissonance but not its perceived tension. *Scientific reports*, 10(1):1–11, 2020. Publisher: Nature Publishing Group.
- [41] German language has four cases: nominative (subject), accusative (direct object), dative (indirect object), and genitive (possessive).
- [42] Giulio Tononi, Gerald M. Edelman, and Olaf Sporns. Complexity and coherency: integrating information in the brain. *Trends in cognitive sciences*, 2(12):474–484, 1998. Publisher: Elsevier.
- [43] Peter E. Latham and Sheila Nirenberg. Synergy, redundancy, and independence in population codes, revisited. *Journal of Neuroscience*, 25(21):5195–5206, 2005. Publisher: Soc Neuroscience.
- [44] Elad Ganmor, Ronen Segev, and Elad Schneidman. Sparse low-order interaction network underlies a highly correlated and learnable neural population code. *Proceedings of the National Academy of sciences*, 108(23):9679–9684, 2011. Publisher: National Acad Sciences.
- [45] Andrea I. Luppi, Pedro AM Mediano, Fernando E. Rosas, Negin Holland, Tim D. Fryer, John T. O’Brien, James B. Rowe, David K. Menon, Daniel Bor, and Emmanuel A. Stamatakis. A synergistic core for human brain evolution and cognition. *BioRxiv*, 2020. Publisher: Cold Spring Harbor Laboratory.
- [46] Andrea I. Luppi, Pedro AM Mediano, Fernando E. Rosas, Judith Allanson, John D. Pickard, Robin L. Carhart-Harris, Guy B. Williams, Michael M. Craig, Paola Finnoia, and Adrian M. Owen. A synergistic workspace for human consciousness revealed by integrated information decomposition. *BioRxiv*, 2020. Publisher: Cold Spring Harbor Laboratory.
- [47] Fernando E. Rosas, Pedro AM Mediano, Henrik J. Jensen, Anil K. Seth, Adam B. Barrett, Robin L. Carhart-Harris, and Daniel Bor. Reconciling emergences: An information-theoretic approach to identify causal emergence in multivariate data. *PLOS Computational Biology*, 16(12):e1008289, 2020. Publisher: Public Library of Science San Francisco, CA USA.
- [48] Luciano Telesca and Michele Lovullo. Revealing competitive behaviours in music by means of the multifractal detrended fluctuation analysis: application to Bach’s *Sinfonias*. *Proceedings of the Royal Society A: Mathematical, Physical and Engineering Sciences*, 467(2134):3022–3032, 2011. Publisher: The Royal Society Publishing.
- [49] Alfredo González-Espinoza, Hernán Larralde, Gustavo Martínez-Mekler, and Markus Müller. Multiple scaling behaviour and nonlinear traits in music scores. *Royal Society open science*, 4(12):171282, 2017. Publisher: The Royal Society Publishing.
- [50] Alfredo González-Espinoza, Gustavo Martínez-Mekler, and Lucas Lacasa. Arrow of time across five centuries of classical music. *Physical Review Research*, 2(3):033166, 2020. Publisher: APS.
- [51] Conor Finn and Joseph T. Lizier. Pointwise partial information decomposition using the specificity and ambiguity lattices. *Entropy*, 20(4):297, 2018. Publisher: Multidisciplinary Digital Publishing Institute.
- [52] Pedro AM Mediano, Fernando Rosas, Robin L. Carhart-Harris, Anil K. Seth, and Adam B. Barrett. Beyond integrated information: A taxonomy of information dynamics phenomena. *arXiv preprint arXiv:1909.02297*, 2019.